Clinical, Cosmetic and Investigational Dermatology

Dovepress
Taylor & Francis Group

Open Access Full Text Article

ORIGINAL RESEARCH

Mendelian Randomization Combined with Single-Cell Transcriptome Analysis Reveals the Role of the Key Gene PCLAF in the Pathogenesis of Atopic Dermatitis

Rui Tao[1,*], Xuejie Chen[1,*], Yingying Wang[2,*], Sicheng Li[1], Shengzhi Zhou[1], Sis Aghayants[1], Lingling Yan[3], Qi Zhang[4], Zhanyong Zhu[1]

[1]Department of Plastic Surgery, Renmin Hospital of Wuhan University, Wuhan, Hubei Province, 430060, People's Republic of China; [2]Department of Otolaryngology-Head and Neck Surgery, Renmin Hospital of Wuhan University, Wuhan, Hubei Province, 430060, People's Republic of China; [3]Department of Plastic and Cosmetic Surgery, Hubei Provincial Hospital of Traditional Chinese Medicine, Wuhan, Hubei Province, 430061, People's Republic of China; [4]Department of Plastic and Cosmetic Surgery, Tongji Hospital, Tongji Medical College, Huazhong University of Science and Technology, Wuhan, Hubei Province, 430030, People's Republic of China

*These authors contributed equally to this work

Correspondence: Lingling Yan, Department of Plastic and Cosmetic Surgery, Hubei Provincial Hospital of Traditional Chinese Medicine, Wuhan, Hubei Province, People's Republic of China, Email yanll197803@126.com; Zhanyong Zhu, Department of Plastic Surgery, Renmin Hospital of Wuhan University, Wuhan, Hubei Province, People's Republic of China, Email zyzhu@whu.edu.cn

Background: Atopic dermatitis (AD) is a chronic inflammatory skin condition characterized by itching and rashes, influenced by genetic, environmental, and immune factors. Despite significant research, the molecular mechanisms underlying AD are not fully understood. This study aims to integrate single-cell RNA sequencing (scRNA-seq) with Mendelian Randomization (MR) to uncover genetic and metabolic pathways contributing to AD.

Materials and Methods: Data from scRNA-seq and bulk RNA sequencing datasets were analyzed to identify differentially expressed genes. The edgeR package was used for differential expression analysis, and candidate genes were explored using MR, employing eQTL data to determine causal relationships with AD. The inverse variance weighted method facilitated MR analysis, while gene set enrichment analysis (GSEA) was used to identify pathways associated with AD. Single-cell analysis was performed with the Seurat package to explore cellular heterogeneity, and pseudotime and cellular communication analyses were conducted to understand cell differentiation and interactions in AD.

Results: The study identified key genes—PCLAF, MICB, CHAD, and CA4—linked to AD, with PCLAF notably acting as a risk factor. These genes are involved in cell cycle regulation, immune evasion, cell adhesion, and metabolic processes. The MR analysis highlighted lipid, amino acid, and energy metabolism as critical pathways in AD. Single-cell analysis revealed increased cellular communication in AD, especially in Langerhans cells, keratinocytes, and T cells, signifying dysregulated immune responses and inflammatory pathways. Pseudotime analysis indicated abnormal differentiation trajectories in these cell types.

Conclusion: Our study highlights the importance of PCLAF in the pathogenesis of AD, indicating it as a potential target for future therapeutic strategies aimed at alleviating the disease by addressing genetic and metabolic disruptions.

Keywords: atopic dermatitis, Mendelian randomization, single-cell RNA sequencing, gene expression

Introduction

Atopic dermatitis (AD) is a common chronic inflammatory skin disease characterized by severe itching, rashes, and dry skin.[1] The pathogenesis of AD involves a complex interplay of genetic, environmental, and immune system factors.[2] Patients with AD often exhibit a range of immune system dysregulation features, including significantly elevated serum immunoglobulin E (IgE) levels, a predominance of Th2 cytokines, and an increased number of T cells expressing

Received: 30 November 2024
Accepted: 27 March 2025
Published: 8 April 2025

cutaneous lymphocyte-associated antigens.[3] Abnormal metabolism of skin lipids and proteins may disrupt the skin barrier function, making the skin more susceptible to external irritants and allergen penetration, thereby triggering and exacerbating AD.[4] AD affects all age groups, is common in both children and adults, and significantly impairs the quality of daily life.[5] Despite extensive research, the precise molecular mechanisms underlying AD remain elusive, necessitating further exploration into the genetic and metabolic pathways involved in its pathogenesis.[6]

Mendelian Randomization (MR) is an analytical method that uses genetic variations as instrumental variables (IVs) to infer causal relationships between exposures and outcomes.[7] Compared to randomized controlled trials, MR can reduce the interference of confounding factors, avoid reverse causality, and minimize the impact of omitted variable bias.[8] In dermatological research, Gao et al used MR to assess the potential causal relationship between psoriasis and cardiovascular diseases.[9] The findings demonstrated that increased genetic susceptibility to psoriasis is associated with a higher risk of heart failure, atrial fibrillation, myocardial infarction, vascular diseases, and peripheral artery disease. Therefore, by utilizing expression quantitative trait loci (eQTL) data, MR can also be used to identify genetic factors that may contribute to the development of AD, providing a robust framework for elucidating the genetic architecture of AD.[10]

Single-cell RNA sequencing (scRNA-seq) has revolutionized our understanding of cellular heterogeneity and gene expression dynamics at a granular level. The technology enables the profiling of individual cells within a tissue, revealing distinct cellular subpopulations and their specific gene expression patterns.[11,12] With the reduction in sequencing costs and the continuous improvement of analytical tools, scRNA-seq has expanded from its initial focus on transcriptome analysis to a multi-omics level, involving multidimensional integrated analyses such as single-cell proteomics, single-cell metabolomics, and spatial transcriptomics.[13,14] For example, the latest single-cell multi-omics technologies can simultaneously detect gene expression, chromatin states, and protein expression within individual cells, providing a more comprehensive perspective for uncovering the molecular characteristics of cells.[15] In dermatological research, the application of single-cell sequencing technologies has been continuously expanding, offering new insights into understanding the pathogenesis of skin diseases. For example, Liu et al analyzed CD45 immune cells in skin samples from 31 patients using scRNA-seq technology.[16] The study revealed significant transcriptional dysregulation in skin-resident memory T cells in both AD and psoriasis. Alkon et al utilized scRNA-seq and T-cell receptor sequencing technologies to perform a comparative analysis of skin samples from patients with chronic nodular prurigo (CNPG), patients with AD, and healthy controls.[17] The study discovered that both CNPG and AD exhibited characteristics of type 2 immune responses. However, CNPG lacked the strong immune activation pathways commonly observed in AD and was instead characterized by an upregulation of stromal remodeling mechanisms. Therefore, in the context of AD, scRNA-seq allows for the identification of key immune and skin cell types involved in the disease process, providing a detailed map of cellular interactions and gene regulatory networks.[18]

Therefore, this study is aimed at integrating scRNA-seq and MR analyses to uncover the molecular mechanisms driving AD. By combining differential gene expression analysis with eQTL data and conducting MR and gene set enrichment analysis (GSEA), we seek to identify causal genes and metabolic pathways associated with AD. This comprehensive approach not only highlights potential biomarkers and therapeutic targets but also enhances our understanding of AD's complex etiology.

Materials and Methods

Data Source

The scRNA-seq dataset GSE153760 and the bulk datasets GSE193309 and GSE5667 were downloaded from the GEO database (https://www.ncbi.nlm.nih.gov/geo/). GSE153760 included 8 AD cases and 7 controls. GSE193309 included 116 AD cases, 111 adjacent normal skin cases, and 112 healthy controls. GSE5667 included 12 AD cases, 12 adjacent normal skin cases, and 10 healthy controls. The eQTL data was obtained from the SMR website (https://yanglab.westlake.edu.cn/software/smr/#Overview) and downloaded as skin tissue eQTL data (GTEx_Analysis_2017-06-05_v8_WholeGenomeSeq_838Indiv_Analysis_Freeze.lookup_tabletxt.gz). The blood metabolite data was downloaded from the GWAS Catalog (https://www.ebi.ac.uk/gwas/), consisting of GWAS data for 1400 circulating metabolites from European populations (GCST90199621-GCST90201020). The AD GWAS datasets, ebi-a-GCST90027161 and ebi-

a-GCST90018784, were downloaded from the IEU database (https://gwas.mrcieu.ac.uk/). The ebi-a-GCST90027161 dataset included 796,661 samples of European ancestry and 16,121,213 SNPs, while the ebi-a-GCST90018784 dataset included 481,299 samples and 24,185,642 SNPs. The data were analyzed in accordance with the study design (Figure 1).

Differential Gene Analysis

The edgeR package (v.4.0.16) was used to normalize and perform differential expression analysis on the microarray dataset GSE153760. The criteria for selecting differentially expressed genes were set as follows: a. p-value < 0.05; b. |FoldChange| > 0.58.

Mediator Mendelian Randomization Analysis

The eQTLs of differentially expressed genes from the GSE153760 dataset were utilized as the exposure, and AD was the outcome (using two datasets: ebi-a-GCsT90027161and ebi-a-GCsT90018784). The extract_instruments() function from the TwoSampleMR R package (v.0.5.8) was employed to select IVs for the exposure. The selection criteria were set as follows: a. p-value < 5×10^{-6}; b. R2 < 0.001, kb > 1000. The harmonise_data() function from the TwoSampleMR R package (version 0.5.8) was used to align the SNPs of the exposure and outcome. The mr() function, combined with the inverse variance weighted (IVW) method, was employed to conduct MR analysis. A p-value threshold of < 0.05 was used to identify genes that demonstrate a causal relationship with AD. The IVW algorithm provided more precise causal estimates. The random effects model of the IVW method could be used to estimate MR results for exposures with heterogeneity and was sensitive to horizontal pleiotropy. The odds ratio (OR) values of genes obtained through MR from the dataset ebi-a-GCsT90018784 were compared with the up- or down-regulation trends observed in differential analysis. Genes exhibiting consistent trends were retained as candidate genes. Additionally, MR was conducted using the dataset ebi-a-GCST90027161 to validate the reliability of the candidate genes.

Using blood metabolite data (GCST90199621-GCST90201020) as exposure factors and AD as the outcome, IVs were selected based on the following criteria: a. p-value < 5×10^{-8}; b. R2 < 0.001, kb > 1000. The harmonise_data function from the TwoSampleMR R package (v.0.5.8) was employed to align the SNPs of the exposure and outcome. MR analysis

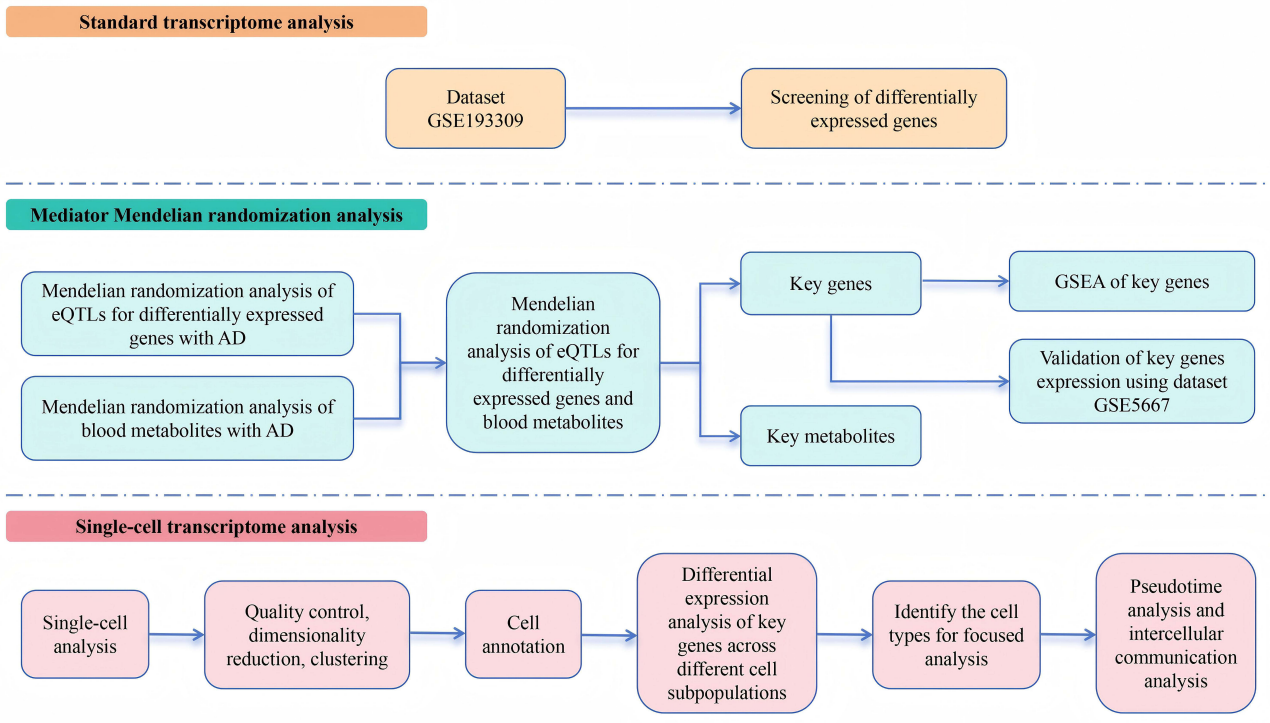

Figure 1 Flowchart of the study.

https://doi.org/10.2147/CCID.S506139

was conducted using the mr() function combined with the IVW method. Metabolites demonstrating a causal relationship with AD were identified based on a p-value < 0.05.

The eQTL data of candidate genes obtained from the aforementioned screening were utilized as the exposure, while the metabolites demonstrating a causal relationship with AD served as the outcome. IVs were selected based on the following criteria: a. p-value < 5×10^{-8}; b. R2 < 0.001, kb > 1000. The harmonise_data function from the TwoSampleMR R package (v.0.5.8) was employed to align the SNPs of the exposure and outcome. MR analysis was conducted using the mr() function combined with the IVW method. Genes exhibiting a causal relationship with metabolites were identified based on a p-value < 0.05.

In the sensitivity analysis, heterogeneity testing was performed using the mr_heterogeneity() function and horizontal pleiotropy testing was performed using the mr_pleiotropy_test() function. All analysis parameters were set to default configurations. In the heterogeneity test results, heterogeneity was considered absent if the Q_pval exceeded 0.05. For exposures exhibiting heterogeneity, the MR effect size was estimated by the random-effects model of the IVW. In the horizontal pleiotropy test, a P-value greater than 0.05 indicated the absence of horizontal pleiotropy. If horizontal pleiotropy was present, the exposure was excluded from subsequent analyses.

To ensure the positive results of the MR analysis were not confounded by reverse causality, the mr_steiger() function was used to conduct the Steiger test. A P-value less than 0.05 indicated the absence of reverse causality between the exposure and the outcome.

GSEA

GSEA was conducted on differential analysis data from GSE193309 utilizing the clusterProfiler package (v.4.10.1) and data sets from the GO and KEGG databases. Pathways containing genes with a causal relationship to AD were identified to explore functions.

Validation of Transcriptional Expression Trends of Key Genes

Conducted differential analysis on genes with a causal relationship to AD by using the external dataset GSE5667. The results were displayed with box plots to examine whether similar trends appeared in other datasets and to evaluate whether the findings were coincidental.

Single-Cell Analysis and Differential Expression of Key Genes Across Various Cell Subpopulations

The Seurat package (version 5.1.0) was employed for quality control and efficient cell screening. The screening criteria for dataset GSE153760 involved filtering out low-quality cells with fewer than 200 or more than 6000 measured genes, and cells with a mitochondrial gene percentage exceeding 15%. Subsequently, the FindVariableFeatures function was utilized to identify the top 2000 highly variable genes within the GSE153760 dataset. Next, the ScaleData and RunPCA functions were used to determine the number of principal components (PCs) based on the Seurat object. The number of PCs was set to 30 to generate cell clusters, and the results were visualized by using a UMAP plot. To annotate the cell clusters, unsupervised clustering was performed by using the FindClusters and FindNeighbors functions. The clearest clustering results were obtained when the resolution was set to 0.8. Cell types were annotated based on marker genes as follows: macrophages were marked with the gene CD14, Langerhans cells (LCs) with the gene D207, T cells with the gene FOXP3, keratinocytes (KCs) with the genes KRT5 and KRT1, melanocytes with the gene PMEL, mast cells with the gene TPSAB1, fibroblasts with the gene COL1A1, endothelial cells with the genes PECAM1 and CD31, plasmacytoid dendritic cells with the gene LILRA4, lymphatic endothelial cells with the genes CCL21 and LYVE1, dendritic cells with the genes CD1A and CD1C, and NK T cells with the genes GZMB and NKG7. These markers were referenced from Rindler et al (Spontaneously Resolved Atopic Dermatitis Shows Melanocyte and Immune Cell Activation Distinct From Healthy Control Skin).[19]

The DotPlot function was used to display the distribution and expression of selected genes across cells. Differential genes in the GSE153760 dataset were identified by using the FindMarkers function from the Seurat package, with an

adjusted p-value threshold of less than 0.05 for selection. Violin plots were used to display the expression and differential of key genes in cells as identified by the mediation MR analysis.

Pseudotemporal Analysis

To identify distinct trajectories representing cellular pseudotime pathways, the Monocle2 R package (v.2.30.1) was used to extract T cells, LCs, and KCs. Subsequently, a Monocle object was created using the newCellDataSet function. Differentially expressed genes were identified by using the differentialGeneTest function and the setOrderingFilter function. Finally, the reduceDimension function and the orderCells function were utilized to perform dimensionality reduction on the data and to order the cells based on pseudotime.

Cellular Communication Analysis

Cellular communication analysis was conducted on single-cell subpopulations derived from pseudotime using the CellChat package (version 2.1.2). The scRNA-seq dataset GSE153760 was divided into AD and normal groups based on sample information, and cellular communication analysis was performed separately for each group. Utilizing the human cell communication database CellChatDB.human and removing non-protein signals from the database, the study calculated intercellular communication probabilities and networks using the triMean method within the computeCommunProb function of the CellChat package. Intercellular communications involving fewer than 10 cells were filtered out, and only ligand-receptor interactions with a p-value less than 0.05 were considered to predict intercellular interactions among various cell types.

Results

Differentially Expressed Genes

Differential analysis of the dataset GSE193309 was conducted using the edgeR package, with genes selected based on |log2FC| greater than 0.58 and a p-value less than 0.05. The analysis identified 1826 upregulated and 1603 downregulated genes (Table S1). The results were visually represented using volcano plots and heat maps (Figure 2).

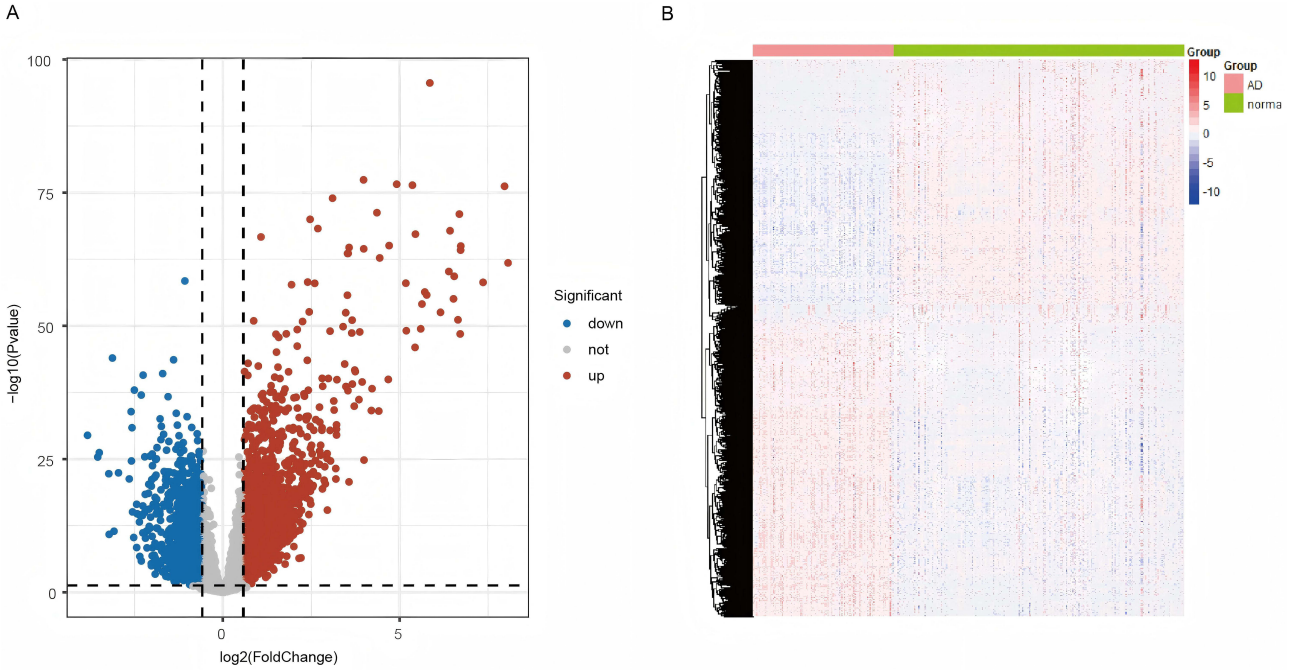

Figure 2 Differential expression between AD and Normal in the GSE193309 dataset. (**A**) Volcano plot. (**B**) Heat map.

https://doi.org/10.2147/CCID.S506139

Mediation Mendelian Randomization Analysis

By integrating differentially expressed genes with eQTL data, the study identified 1874 candidate genes. A two-sample MR analysis using eQTLs of candidate genes as genetic IVs and AD as the outcome identified 136 genes with a causal relationship to AD in the dataset ebi-a-GCST90018784. The ORs of the MR-identified genes were compared with trends from differential expression analysis, and genes with consistent trends were retained. Ultimately, 4 differentially expressed genes (CA4, MICB, CHAD, PCLAF) were identified as candidate genes causally associated with AD (Figure 3A, Table S2). To ensure the reliability of the candidate genes, another MR analysis was conducted using the AD dataset ebi-a-GCST90027161. The results demonstrated that the causal relationships for the 4 candidate genes remained significant and aligned with the causal directions observed in the previous MR analysis (Figure 3B).

A two-sample MR analysis was conducted using blood metabolite data (GCST90199621-GCST90201020) as exposures and AD datasets (ebi-a-GCST90027161, ebi-a-GCST90018784) as outcomes. The MR results identified 2952 metabolites in dataset ebi-a-GCST90018784 and 3046 metabolites in dataset ebi-a-GCST90027161 with causal relationships to AD. After intersecting the metabolites from both analyses and screening based on OR value direction, 99 circulating metabolites with causal relationships to AD were identified (Tables S3 and S4).

Finally, a two-sample MR analysis was conducted on the 4 differentially expressed genes and 99 metabolites, identifying 29 metabolites with causal relationships to the 4 genes (Table S5). Based on the genes and metabolites

A

exposure	outcome	nsnp	method	pval	OR(95% CI)
MICB	ebi-a-GCST90018784	3	Inverse variance weighted	0.039	1.033 (1.002 to 1.066)
CA4	ebi-a-GCST90018784	2	Inverse variance weighted	0.034	1.179 (1.013 to 1.372)
CHAD	ebi-a-GCST90018784	2	Inverse variance weighted	0.012	0.811 (0.689 to 0.955)
PCLAF	ebi-a-GCST90018784	3	Inverse variance weighted	0.001	1.607 (1.206 to 2.143)

B

exposure	outcome	nsnp	method	pval	OR(95% CI)
MICB	ebi-a-GCST90027161	3	Inverse variance weighted	<0.001	1.042 (1.019 to 1.066)
CA4	ebi-a-GCST90027161	2	Inverse variance weighted	0.002	1.186 (1.065 to 1.321)
CHAD	ebi-a-GCST90027161	2	Inverse variance weighted	0.009	0.844 (0.743 to 0.959)
PCLAF	ebi-a-GCST90027161	3	Inverse variance weighted	0.008	1.121 (1.030 to 1.221)

C

exposure	outcome	nsnp	method	pval	OR(95% CI)
Oxalate (ethanedioate) levels	ebi-a-GCST90018784	54	Inverse variance weighted	<0.001	0.887 (0.844 to 0.934)
1-(1-enyl-palmitoyl)-2-oleoyl-GPE (p-16:0/18:1) levels	ebi-a-GCST90018784	7	Inverse variance weighted	<0.001	1.275 (1.141 to 1.425)
Docosahexaenoylcarnitine (C22:6) levels	ebi-a-GCST90018784	73	Inverse variance weighted	<0.001	1.855 (1.794 to 1.919)
Tetrahydrocortisol glucuronide levels	ebi-a-GCST90018784	82	Inverse variance weighted	<0.001	0.896 (0.865 to 0.928)
4-hydroxyphenylpyruvate levels	ebi-a-GCST90018784	62	Inverse variance weighted	0.002	1.056 (1.021 to 1.094)
Adenosine 5'-diphosphate (ADP) to glycine ratio	ebi-a-GCST90018784	95	Inverse variance weighted	<0.001	0.869 (0.853 to 0.886)
Serine to alpha-ketobutyrate ratio	ebi-a-GCST90018784	20	Inverse variance weighted	0.003	0.891 (0.826 to 0.961)

D

exposure	outcome	nsnp	method	pval	OR(95% CI)
Oxalate (ethanedioate) levels	ebi-a-GCST90027161	54	Inverse variance weighted	<0.001	0.904 (0.876 to 0.933)
1-(1-enyl-palmitoyl)-2-oleoyl-GPE (p-16:0/18:1) levels	ebi-a-GCST90027161	7	Inverse variance weighted	<0.001	1.407 (1.304 to 1.519)
Docosahexaenoylcarnitine (C22:6) levels	ebi-a-GCST90027161	72	Inverse variance weighted	<0.001	1.438 (1.406 to 1.471)
Tetrahydrocortisol glucuronide levels	ebi-a-GCST90027161	81	Inverse variance weighted	<0.001	0.916 (0.894 to 0.939)
4-hydroxyphenylpyruvate levels	ebi-a-GCST90027161	62	Inverse variance weighted	<0.001	1.191 (1.164 to 1.218)
Adenosine 5'-diphosphate (ADP) to glycine ratio	ebi-a-GCST90027161	97	Inverse variance weighted	<0.001	0.958 (0.947 to 0.970)
Serine to alpha-ketobutyrate ratio	ebi-a-GCST90027161	20	Inverse variance weighted	<0.001	0.862 (0.820 to 0.907)

E

exposure	outcome	nsnp	method	pval	OR(95% CI)
MICB	Docosahexaenoylcarnitine (C22:6) levels	3	Inverse variance weighted	0.041	1.040 (1.002 to 1.080)
CA4	Oxalate (ethanedioate) levels	2	Inverse variance weighted	0.026	0.826 (0.699 to 0.977)
CHAD	Tetrahydrocortisol glucuronide levels	2	Inverse variance weighted	<0.001	1.203 (1.083 to 1.335)
PCLAF	1-(1-enyl-palmitoyl)-2-oleoyl-GPE (p-16:0/18:1) levels	3	Inverse variance weighted	0.030	1.177 (1.016 to 1.364)
PCLAF	4-hydroxyphenylpyruvate levels	3	Inverse variance weighted	0.004	1.251 (1.075 to 1.457)
PCLAF	Adenosine 5'-diphosphate (ADP) to glycine ratio	3	Inverse variance weighted	0.008	0.761 (0.623 to 0.930)
PCLAF	Serine to alpha-ketobutyrate ratio	3	Inverse variance weighted	0.026	0.843 (0.725 to 0.980)

Figure 3 Results of the MR analysis between gene eQTL and AD (ebi-a-GCST90018784) (**A**), gene eQTL and AD (ebi-a-GCST90027161) (**B**), circulating metabolites with mediating effects and AD (ebi-a-GCST90018784) (**C**), circulating metabolites with mediating effects and AD (ebi-a- GCST90027161) (**D**), and 4 genes and 7 circulating metabolites with mediating effects (**E**).

obtained from multiple MR analyses, mediation causal relationships were constructed. Ultimately, 7 definitive mediation causal relationships were identified, involving 4 genes and 7 metabolites.

The gene CHAD served as a protective factor for AD, whereas the genes CA4, PCLAF, and MICB were identified as risk factors for AD (Figure 3A and B). Among the 7 metabolites, the levels of 1-(1-enyl-palmitoyl)-2-oleoyl-GPE, docosahexaenoylcarnitine, and 4-hydroxyphenylpyruvate were identified as risk factors for AD (OR > 1), whereas the levels of tetrahydrocortisol glucuronide, oxalate, the serine to alpha-ketobutyrate ratio, and the Adenosine 5'-diphosphate (ADP) to glycine ratio were found to be protective factors for AD (Figure 3C and D). The gene PCLAF was a risk factor for the metabolites 1-(1-enyl-palmitoyl)-2-oleoyl-GPE and 4-hydroxyphenylpyruvate, but a protective factor for the ADP to glycine ratio and the serine to alpha-ketobutyrate ratio. The gene MICB was a risk factor for docosahexaenoylcarnitine levels, while the gene CA4 was protective for Oxalate levels. Additionally, the gene CHAD was a risk factor for tetrahydrocortisol glucuronide levels (Figure 3E).

Sensitivity tests for key genes and key metabolites did not reveal heterogeneity or horizontal pleiotropy (Tables S6-S15). Reverse causality tests indicated that there was no reverse causal relationship between exposure and outcome in all MR analyses (Tables S16-S20).

Exploration of Causal Metabolites

According to the original studies of the metabolites, the levels of metabolites such as 1-(1-enyl-palmitoyl)-2-oleoyl-GPE, docosahexaenoylcarnitine, and tetrahydrocortisol glucuronide can influence lipid metabolism.[20] Oxalate levels impact cofactor and vitamin metabolism, while 4-hydroxyphenylpyruvate levels affect amino acid metabolism. The shared enzymes or transport proteins between ADP and glycine include trifunctional purine biosynthesis protein adenosine-3 and glutathione synthetase, both involved in energy metabolism.[21,22] Similarly, the shared enzymes or transport proteins between serine and alpha-ketobutyrate include L-serine dehydratase, L-threonine deaminase, both involved in amino acid metabolism.[23,24] Based on the results of the mediation MR analysis, we found that PCLAF influenced the risk of AD development by affecting various metabolites involved in lipid, amino acid, and energy metabolism. The genes MICB and CHAD influenced AD by impacting lipid metabolism, while the gene CA4 played a role in the pathogenesis of AD by interfering with cofactor and vitamin metabolism.

GSEA

Key genes (CA4, MICB, CHAD, PCLAF) were primarily enriched in 62 GO pathways, including defense response to symbiont, negative regulation of response to biotic stimulus, response to virus, and T cell activation, as well as in 2 KEGG pathways: Natural killer cell mediated cytotoxicity and Kaposi sarcoma-associated herpesvirus infection (Figure 4A and B, Table S21). The study found that key genes were highly associated with pro-inflammatory and immune pathways, potentially causing inflammation and immune response disorders by affecting related pathways, thereby contributing to the progression of AD.

Analysis of the Transcriptome Expression Trends of Key Genes

The external validation dataset GSE5667 was used to verify the transcriptome expression trends of the key genes CA4, MICB, CHAD, and PCLAF. Notably, PCLAF was significantly upregulated in AD, consistent with the differential results observed in dataset GSE193309 (Figure 4C and D). Thus, subsequent research focused on exploring the functions of PCLAF. The PCLAF participated in various cellular processes, including cell cycle regulation, DNA replication, DNA repair, and cell survival.[25] PCLAF could promote the G1/S cell cycle progression in neuroblastoma through the E2F1/PTTG1 axis.[26] Additionally, knocking down PCLAF inhibited glioma progression and glycolysis by inactivating the PI3K/AKT/mTOR pathway.[27] These findings were consistent with the results of our MR analysis, which indicated that PCLAF was associated with inflammatory response and energy metabolism.

Single-Cell Annotation

The scRNA-seq data from 8 AD patients and 7 normal controls in the GSE153760 dataset were utilized to reveal the intrinsic cellular heterogeneity within skin tissues. After excluding low-quality cells with fewer than 200 measured genes,

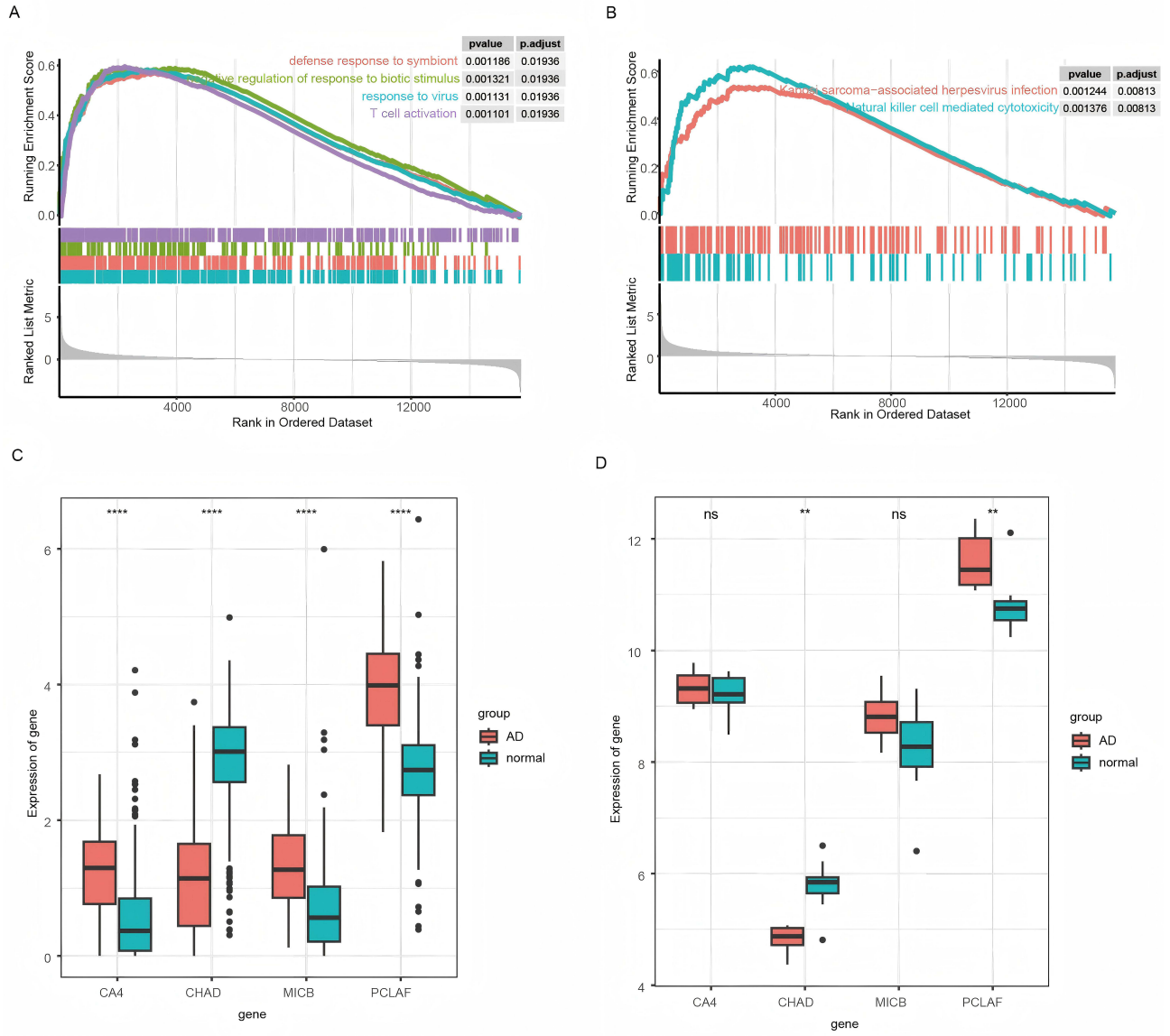

Figure 4 GSEA and transcriptome differential expression analysis. GSEA of key genes based on GO pathways (**A**), based on KEGG pathways (**B**). Differential expression of key genes in the transcriptome dataset GSE193309 (**C**), and in the transcriptome dataset GSE5667 (**D**).
Notes: In the gene differential expression statistical graphs, **P-value < 0.01; ****P-value < 0.0001.

more than 6000 measured genes, or over 15% mitochondrial genes, 44,070 cells were selected for further analysis. By applying PCA dimensionality reduction with the top 30 PCs and setting the resolution to 0.8 for unsupervised clustering, 26 cell clusters were identified (Figure 5A). Based on marker genes identified in previous studies, detailed cell types were determined and annotated, including 13 types: smooth muscle cells (ACTA2), macrophages (CD14), LCs (D207), T cells (FOXP3), KCs (KRT5, KRT1), melanocytes (PMEL), mast cells (TPSAB1), fibroblasts (COL1A1), endothelial cells (PECAM1, CD31), plasmacytoid dendritic cells (LILRA4), lymphatic endothelial cells (CCL21, LYVE1), dendritic cells (CD1A, CD1C), and NK T cells (GZMB, NKG7) (Figure 5B). Based on the distribution of cell subpopulations in disease and control samples, LCs and KCs exhibited a significant increase in the disease samples. Additionally, T cells, dendritic cells, macrophages, and other immune cells also showed an increase (Figure 5C).

In patients with AD, LCs proliferate faster and KCs secrete more chemokines, impacting the Th2 cell-dominated immune response.[28,29] Keratinocyte-derived cytokine thymic stromal lymphopoietin (TSLP) promotes T cell

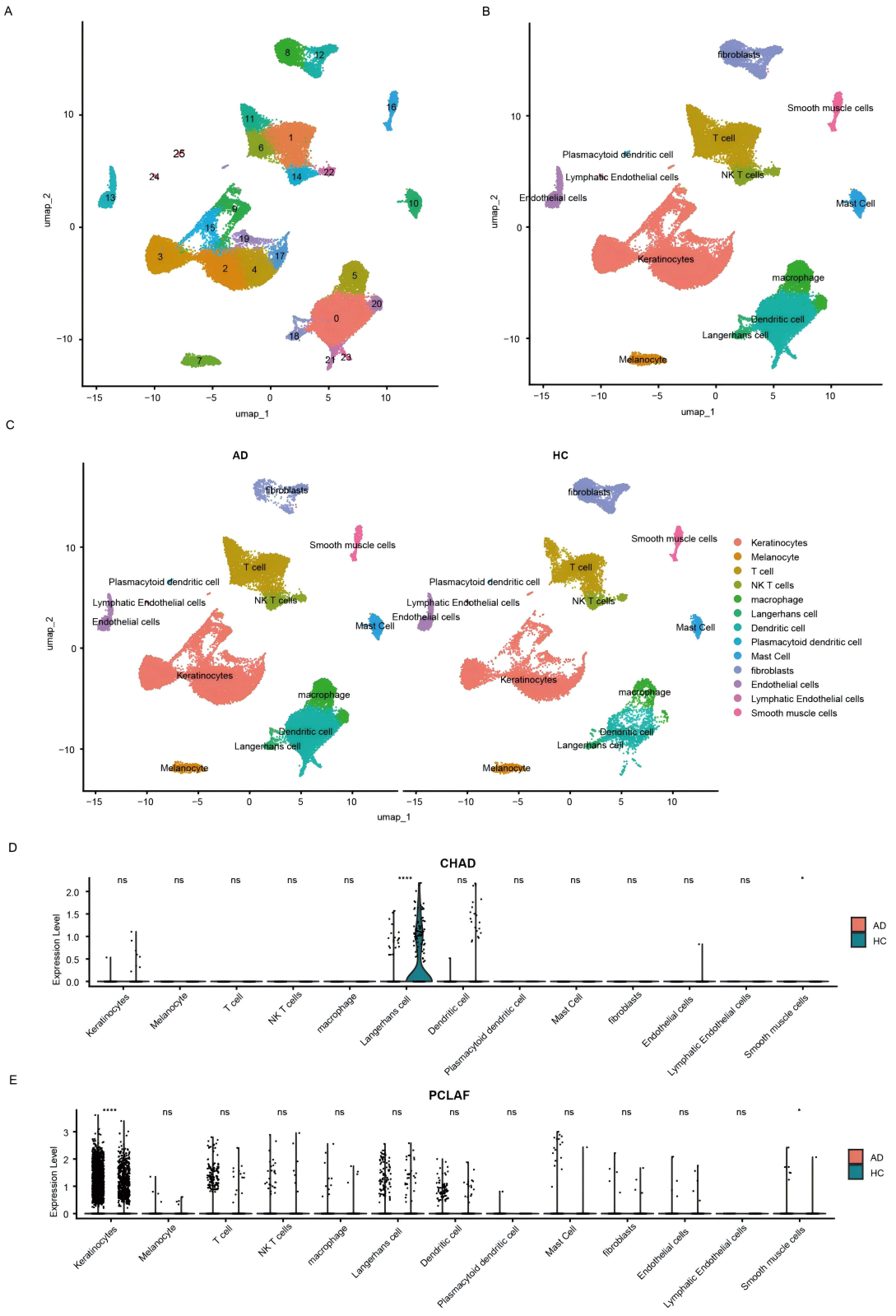

Figure 5 Single-cell clustering in AD and the differential expression of key genes in various cell subpopulations. (**A**) The UMAP clustering plot of the unsupervised clustering of the single-cell dataset GSE153760. (**B**) The UMAP clustering plot showing the distribution of cell subpopulations in the single-cell dataset GSE153760. (**C**) The UMAP clustering plot illustrating the distribution of cell subpopulations based on disease and control samples. (**D**) The expression levels and differential expression of the gene Chad in various cell subpopulations. (**E**) The expression levels and differential expression of the gene PCLAF in various cell subpopulations.
Notes: In the expression trend graphs, *P-value < 0.05; ****P-value < 0.0001.

https://doi.org/10.2147/CCID.S506139

differentiation, with the production of follicular helper T cells (TFH) closely linked to humoral immunity and the severity of AD.[30] Regulating the proliferation of LCs and KCs may be effective in treating AD, but the mechanisms of LCs and KCs proliferation in AD remain unclear.[31]

The study examined the differences in key genes across various cell types. The PCLAF gene was widely expressed, with the highest expression in KCs. The CHAD gene exhibited high expression and significant differences in LCs (Figures 5D, E and S1). Considering the importance of LCs, KCs, and T cells in the pathogenesis of AD, as well as the differential expression of PCLAF and CHAD in various cell subpopulations, LCs, KCs, and T cells were selected as key cells for subsequent analysis.

Pseudotime Analysis

Pseudotime analysis was conducted on LCs, KCs, and T cells (Figure 6). The pseudotime analysis results indicated that the differentiation trajectories of both LCs and KCs exhibited a trend from right to left and bottom to top, whereas the differentiation trajectory of T cells showed a trend from right to left and top to bottom. Additionally, compared to normal samples, LCs, KCs, and T cells demonstrated an elevated level of differentiation in disease specimens. Notably, the differentiation of T cells into Tfh cells is closely associated with humoral immunity and the severity of AD disease.[32,33] The process is significantly influenced by the interaction with KCs and LCs.[34] The regulation of cell proliferation and cell cycle is closely related to cell differentiation.[35,36] Therefore, we hypothesize that PCLAF may influence the differentiation of LCs, KCs, and T cells by regulating the cell cycle and cell proliferation.

Single-Cell Communication

In AD, the cell communication of endothelial cells (AD: 564, HC: 485), dendritic cells (AD: 352, HC: 281), fibroblasts (AD: 292, HC: 163), KCs (AD: 292, HC: 163), LCs (AD: 316, HC: 240), lymphatic endothelial cells (AD: 277, HC: 203), macrophages (AD: 344, HC: 207), mast cells (AD: 62, HC: 44), melanocytes (AD: 255, HC: 148), NK T cells (AD: 257, HC: 248), plasmacytoid dendritic cells (AD: 247, HC: 223), smooth muscle cells (AD: 280, HC: 148), and T cells (AD: 394, HC: 350) was significantly higher than that of normal controls (Tables S22 and S23). LCs are bone marrow-derived antigen-processing and presenting cells primarily located in the basal layer of the epidermis.[37] LCs exhibit increased communication with other cells in AD patients. The results indicated that AD patients exhibited immune dysregulation, characterized by reduced immune-related and increased inflammation-related communication between LCs and other cells compared to normal controls. CTLA4 is a protein that transmits inhibitory signals to T cells.[38] The occurrence of CD86-CTLA4 interactions between LCs and T cells in patients with AD suggested that the condition might have disrupted the epidermal immune response (Figure 7A and B).

KCs not only resist damage caused by environmental factors but also participate in the innate immune response and skin inflammatory reactions.[39] The results showed increased communication between KCs and other cells compared to normal controls. LAMB3-CD44 channels increased significantly. The LAMB3 gene encodes the laminin β3 subunit, a member of the laminin family closely associated with skin structural integrity.[40] Alterations in the LAMB3 gene can result in blistering skin lesions, affecting the skin barrier function.[41] Metabolic pathways associated with ITGA and ITGB are increased in AD patients. Due to the association of the ITGA and ITGB families with the PI3K/Akt pathway, where AKT signaling primarily acts as an inhibitor of apoptosis, KCs in AD patients may exhibit excessive proliferation[42] (Figure 7C and D).

Communication between T cells and other cells was increased in AD patients. Compared to normal controls, T cell immune and inflammation-related communications were elevated, indicating dysregulated T cell metabolism and immune imbalance (Figure 7E and F).

Discussion

As a common inflammatory skin disease, AD currently has an incompletely understood etiology.[43] The application of MR enables researchers to integrate eQTL and GWAS, providing a more scientific and precise method for identifying genes associated with disease risk.[44] The scRNA-seq technology, capable of revealing cellular heterogeneity, developmental trajectories, and complex intercellular interactions, offers new perspectives for exploring disease mechanisms.[45] This study employed a comprehensive approach integrating scRNA-seq, MR, and GSEA to decipher the molecular

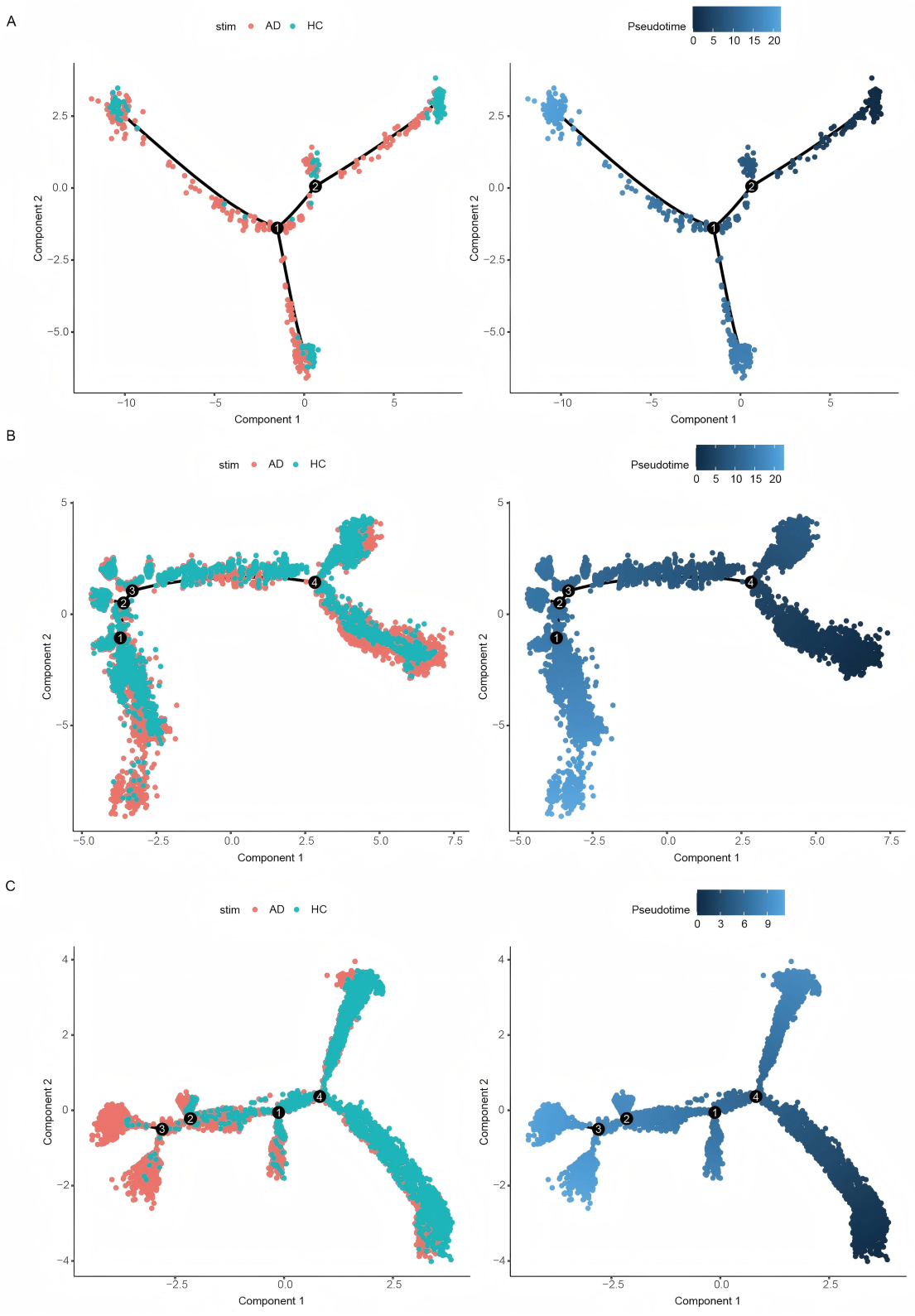

Figure 6 UMAP plot of pseudotime analysis for LCs (**A**), KCs (**B**), and T cells (**C**).
Note: In the cell differentiation trajectory plot on the right side, lighter shades of blue indicate a higher degree of differentiation.

https://doi.org/10.2147/CCID.S506139

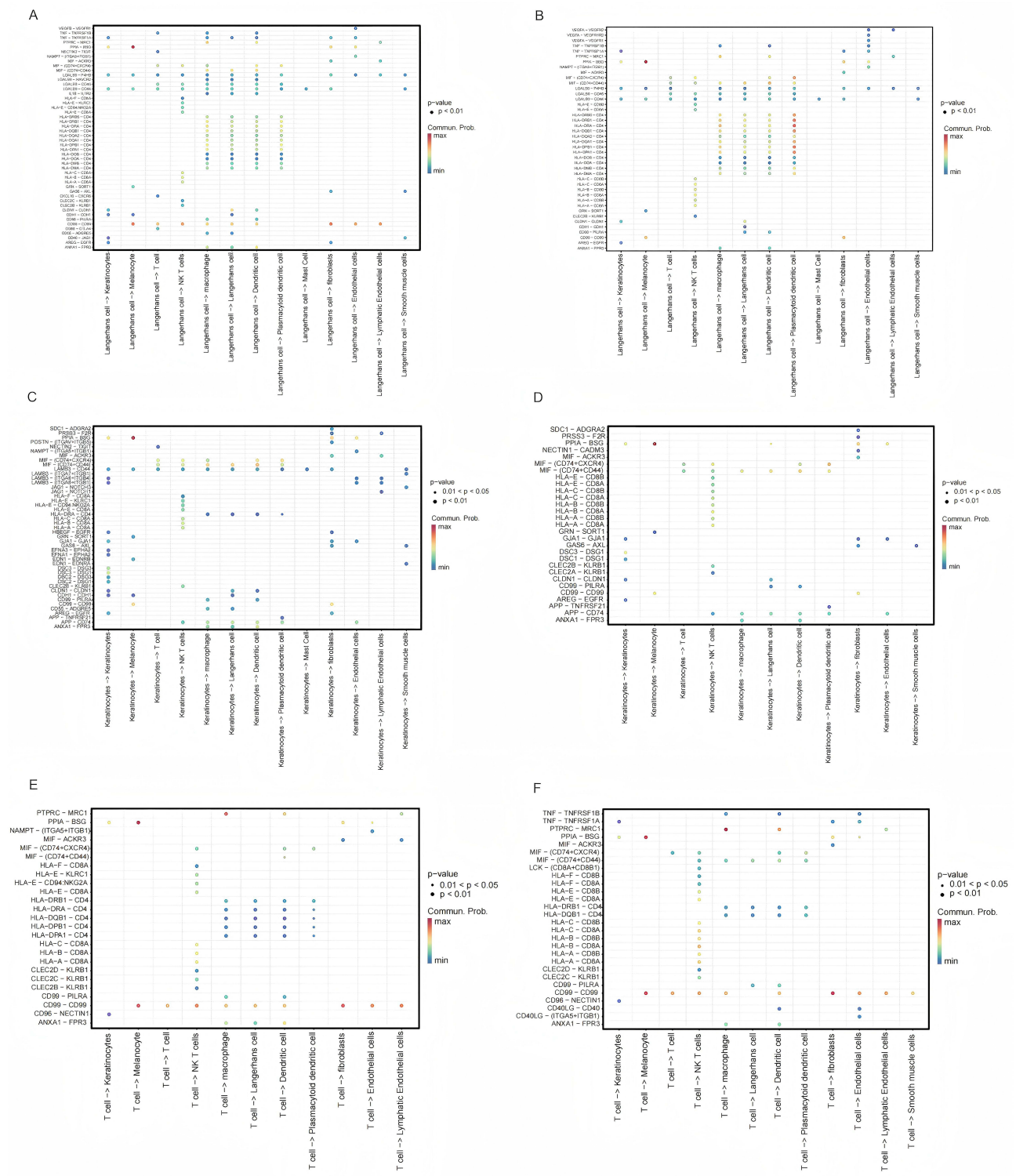

Figure 7 Cellular communication analysis. Bubble chart of cellular communication in LCs of the AD group (**A**), in LCs of the HC group (**B**), in KCs of the AD group (**C**), in KCs of the HC group (**D**), in T cells of the AD group (**E**), and in T cells of the HC group (**F**).

mechanisms underlying AD condition. By combining differential gene expression analysis with eQTL data, we identified potential causal relationships between specific genes and AD, further reinforced by mediation MR analysis linking key genes to relevant metabolic pathways. This study emphasizes the intricate interaction between genetic variations and metabolic pathways in AD, revealing that specific genes, such as PCLAF, MICB, CHAD, and CA4, significantly

influence disease pathogenesis through distinct metabolic alterations and immune responses. These results offer novel molecular biomarkers for therapeutic intervention in AD management.

Firstly, our findings revealed the significant role of the PCLAF, MICB, CHAD, and CA4 genes in the pathogenesis of AD. The MR analysis highlighted CA4, PCLAF, and MICB as risk factors, while CHAD emerged as a protective factor, aligning with their respective expression trends in AD and control samples. The protein encoded by the PCLAF gene is associated with cell cycle regulation.[46] Through bioinformatics analysis, PCLAF has been identified as a potential regulator of the pathological processes in heart failure, glioblastoma, and prostate cancer, highlighting the potential of PCLAF as a therapeutic target.[47–49] The protein encoded by the MICB gene is instrumental in facilitating immune evasion.[50] Some studies have found that MICB may play a protective role in the development of childhood asthma.[51] Higher MICB levels are associated with a lower risk of childhood asthma, but they may also increase the risk of gastrointestinal diseases and endocrine-metabolic disorders. Moreover, the MICB gene has been identified as a susceptibility locus for cutaneous lupus erythematosus and is frequently overexpressed in patients with systemic lupus erythematosus (SLE).[52,53] MICB can promote an excessive immune response by binding to the NKG2D receptor, thereby exacerbating the inflammatory process in SLE. The chondroadherin encoded by the CHAD gene participates in cell adhesion and migration.[54] The CA4 gene encodes an enzyme called carbonic anhydrase IV, which is involved in pH regulation, ion transport, gas exchange, and other related processes.[55] In inflammatory bowel disease (IBD) models, the expression and enzymatic activity of CA4 are elevated, and inhibition of CA4 can alleviate the persistent pain associated with IBD.[55] The association between these genes and specific metabolites, such as Docosahexaenoylcarnitine and Tetrahydrocortisol glucuronide, offers new insights into the metabolic dysregulations in AD, suggesting that lipid and energy metabolism disorders may be pivotal in disease progression.

The single-cell analysis revealed altered cellular compositions and enhanced cellular communications in AD, particularly among LCs, KCs, and T cells. These findings are crucial as they highlight the dysregulated immune landscape and the exacerbated inflammatory responses in AD. Additionally, the GSEA results linked the identified genes to immune and inflammatory pathways, reinforcing the notion that immune dysregulation is a hallmark of AD pathophysiology.

The use of MR provided a robust framework for inferring causality from observational data, minimizing confounding biases typically present in epidemiological studies. However, the reliance on publicly available eQTL datasets and predefined statistical thresholds might limit the discovery of novel genetic associations. Moreover, while scRNA sequencing offers detailed insights into cellular heterogeneity, the interpretation of such complex data requires careful consideration of technical and biological noise. This study integrated multi-omic data layers and advanced analytical techniques, representing a significant advancement in understanding the complex biology of AD. The utilization of MR to validate causal relationships between genes, metabolites, and disease phenotypes ensures a higher confidence in the results, potentially guiding targeted therapeutic strategies. Furthermore, the extensive dataset comprising both single-cell and bulk RNA sequences provides a comprehensive view of the molecular alterations in AD.

Lastly, while this study provides valuable insights, it still faces some obstacles worth further consideration. First, the datasets used in this study were all derived from specific public databases. Since the sample sources of these datasets may have certain regional and population limitations, particularly with GWAS data predominantly based on European populations, the use of such data may introduce selection bias and fail to fully represent the genetic characteristics and disease associations of other populations. Future studies should consider incorporating data from diverse regions and ethnic groups to enhance the generalizability and applicability of the findings. Secondly, although single-cell analysis technology provides us with a detailed perspective on cellular heterogeneity, data analysis is hindered by various technical and biological biases, adding complexity and uncertainty. Finally, this study primarily focused on the association between specific genes and the onset of AD, without delving into the relationship between these genes and the severity of AD or their interactions with other comorbid conditions. Furthermore, the functional roles of the identified genes and metabolites in the pathogenesis of AD require further experimental validation in future studies. Prospective studies should also explore the therapeutic potential targeting these metabolic pathways, providing new targets for AD treatment.

Conclusion

Through MR combined with single-cell transcriptome analysis, we identified a key gene, PCLAF, that is highly associated with AD. The primary function of PCLAF is to regulate the cell cycle and cell proliferation. The study identified PCLAF as a risk factor for AD. PCLAF interfered with lipid, amino acid, and energy metabolism by affecting various metabolites, thereby increasing the risk of AD. Based on the MR results from this study, the pseudotemporal analysis of LCs, KCs, and T cells in AD patients, and cell communication findings, we hypothesized that PCLAF promoted cell proliferation and interfered with cell differentiation through its intrinsic functions. Additionally, PCLAF may have further disrupted key biological processes in AD patients, such as immune response, inflammation, and cell proliferation, by affecting metabolites in various metabolic pathways. The disruption of these biological processes might have been related to the pathogenesis of AD. In summary, our study highlights the importance of PCLAF in the pathogenesis of AD, indicating it as a potential target for future therapeutic strategies aimed at alleviating the disease by addressing genetic and metabolic disruptions.

Abbreviations

ADP, adenosine 5'-diphosphate; AD, atopic dermatitis; CNPG, chronic nodular prurigo; Eqtl, expression quantitative trait loci; GSEA, gene set enrichment analysis; IBD, inflammatory bowel disease; IgE, immunoglobulin E; IVs, instrumental variables; IVW, inverse variance weighted; KCs, keratinocytes; LCs, Langerhans cells; MR, Mendelian randomization; OR, odds ratio; PCLAF, PCNA clamp-associated factor; PCs, principal components; PCNA, proliferating cell nuclear antigen; scRNA-seq, single-cell RNA sequencing; SLE, systemic lupus erythematosus; TFH, follicular helper T cells; TSLP, thymic stromal lymphopoietin.

Data Sharing Statement

The scRNA-seq dataset GSE153760 and the bulk datasets GSE193309 and GSE5667 were downloaded from the GEO database (https://www.ncbi.nlm.nih.gov/geo/). The eQTL data was obtained from the SMR website (https://yanglab.westlake.edu.cn/software/smr/#Overview) and downloaded as skin tissue eQTL data (GTEx_Analysis_2017-06-05_v8_WholeGenomeSeq_838Indiv_Analysis_Freeze.lookup_tabletxt.gz). The blood metabolite data (GCST90199621-GCST90201020) was downloaded from the GWAS Catalog (https://www.ebi.ac.uk/gwas/). The AD GWAS datasets, ebi-a-GCST90027161 and ebi-a-GCST90018784, were downloaded from the IEU database (https://gwas.mrcieu.ac.uk/).

Ethics Statement

This study utilized publicly available data from open-access databases, and no new human data were collected or generated. According to national legislation in China, specifically Item 1 and Item 2 of Article 32 of the Measures for Ethical Review of Life Science and Medical Research Involving Human Subjects (effective February 18, 2023), research involving publicly available data does not require additional ethical approval or informed consent. Therefore, this study is exempt from review by an Institutional Review Board (IRB).

Acknowledgment

Rui Tao, Xuejie Chen and Yingying Wang are co-first authors for this study. We thank the institute for providing the funding and the individuals for offering help during the manuscript process.

Author Contributions

All authors made a significant contribution to the work reported, whether that is in the conception, study design, execution, acquisition of data, analysis and interpretation, or in all these areas; took part in drafting, revising or critically reviewing the article; gave final approval of the version to be published; have agreed on the journal to which the article has been submitted; and agree to be accountable for all aspects of the work.

Funding

This work was supported by the Industry-University-Research Innovation Fund for Chinese Universities (2021ITA03006; 2020ITA03006).

Disclosure

The authors report no conflicts of interest in this work.

References

1. Quan VL, Erickson T, Daftary K, Chovatiya R. Atopic dermatitis across shades of skin. *Am J Clin Dermatol*. 2023;24(5):731–751. doi:10.1007/s40257-023-00797-1
2. Sroka-Tomaszewska J, Trzeciak M. Molecular mechanisms of atopic dermatitis pathogenesis. *Int J mol Sci*. 2021;22(8):4130. doi:10.3390/ijms22084130
3. Yang G, Seok JK, Kang HC, Cho YY, Lee HS, Lee JY. Skin barrier abnormalities and immune dysfunction in atopic dermatitis. *Int J mol Sci*. 2020;21(8):2867. doi:10.3390/ijms21082867
4. Chovatiya R, Paller AS. JAK inhibitors in the treatment of atopic dermatitis. *J Allergy Clin Immunol*. 2021;148(4):927–940. doi:10.1016/j.jaci.2021.08.009
5. Gatmaitan JG, Lee JH. Challenges and future trends in atopic dermatitis. *Int J mol Sci*. 2023;24(14):11380. doi:10.3390/ijms241411380
6. Vestergaard C, Skovsgaard C, Johansen C, Deleuran M, Thyssen JP. Treat-to-target in atopic dermatitis. *Am J Clin Dermatol*. 2024;25(1):91–98. doi:10.1007/s40257-023-00827-y
7. Birney E. Mendelian randomization. *Cold Spring Harb Perspect Med*. 2022;12(4):a041302. doi:10.1101/cshperspect.a041302
8. Larsson SC, Butterworth AS, Burgess S. Mendelian randomization for cardiovascular diseases: principles and applications. *Eur Heart J*. 2023;44(47):4913–4924. doi:10.1093/eurheartj/ehad736
9. Gao N, Kong M, Li X, et al. The association between psoriasis and risk of cardiovascular disease: a Mendelian randomization analysis. *Front Immunol*. 2022;13:918224. doi:10.3389/fimmu.2022.918224
10. Budu-Aggrey A, Kilanowski A, Sobczyk MK, et al. European and multi-ancestry genome-wide association meta-analysis of atopic dermatitis highlights importance of systemic immune regulation. *Nat Commun*. 2023;14(1):6172. doi:10.1038/s41467-023-41180-2
11. Balzer MS, Ma Z, Zhou J, Abedini A, Susztak K. How to get started with single cell RNA sequencing data analysis. *J Am Soc Nephrol*. 2021;32(6):1279–1292. doi:10.1681/ASN.2020121742
12. Cheng C, Chen W, Jin H, Chen X. A review of single-cell RNA-seq annotation, integration, and cell-cell communication. *Cells*. 2023;12(15):1970. doi:10.3390/cells12151970
13. Lee J, Hyeon DY, Hwang D. Single-cell multiomics: technologies and data analysis methods. *Exp mol Med*. 2020;52(9):1428–1442. doi:10.1038/s12276-020-0420-2
14. Wu X, Yang X, Dai Y, et al. Single-cell sequencing to multi-omics: technologies and applications. *Biomark Res*. 2024;12(1):110. doi:10.1186/s40364-024-00643-4
15. Fu Y, Tao J, Liu T, et al. Unbiasedly decoding the tumor microenvironment with single-cell multiomics analysis in pancreatic cancer. *mol Cancer*. 2024;23(1):140. doi:10.1186/s12943-024-02050-7
16. Liu Y, Wang H, Taylor M, et al. Classification of human chronic inflammatory skin disease based on single-cell immune profiling. *Sci Immunol*. 2022;7(70):eabl9165. doi:10.1126/sciimmunol.abl9165
17. Alkon N, Assen FP, Arnoldner T, et al. Single-cell RNA sequencing defines disease-specific differences between chronic nodular prurigo and atopic dermatitis. *J Allergy Clin Immunol*. 2023;152(2):420–435. doi:10.1016/j.jaci.2023.04.019
18. Nishide M, Shimagami H, Kumanogoh A. Single-cell analysis in rheumatic and allergic diseases: insights for clinical practice. *Nat Rev Immunol*. 2024;24(10):1043.
19. Rindler K, Krausgruber T, Thaler FM, et al. Spontaneously resolved atopic dermatitis shows melanocyte and immune cell activation distinct from healthy control skin. *Front Immunol*. 2021;12:630892. doi:10.3389/fimmu.2021.630892
20. Chen Y, Lu T, Pettersson-Kymmer U, et al. Genomic atlas of the plasma metabolome prioritizes metabolites implicated in human diseases. *Nat Genet*. 2023;55(1):44–53. doi:10.1038/s41588-022-01270-1
21. Onidani K, Miura N, Sugiura Y, et al. Possible therapeutic strategy involving the purine synthesis pathway regulated by ITK in tongue squamous cell carcinoma. *Cancers*. 2021;13(13):3333. doi:10.3390/cancers13133333
22. Lapenna D. Glutathione and glutathione-dependent enzymes: from biochemistry to gerontology and successful aging. *Ageing Res Rev*. 2023;92:102066. doi:10.1016/j.arr.2023.102066
23. Katane M, Nakasako K, Yako K, Saitoh Y, Sekine M, Homma H. Identification of an l-serine/l-threonine dehydratase with glutamate racemase activity in mammals. *Biochem J*. 2020;477(21):4221–4241. doi:10.1042/BCJ20200721
24. Wu L, Deng H. Defluorination of 4-fluorothreonine by threonine deaminase. *Org Biomol Chem*. 2020;18(32):6236–6240. doi:10.1039/d0ob01358g
25. Liu X, Cheng C, Cai Y, et al. Pan-cancer analyses reveal the regulation and clinical outcome association of PCLAF in human tumors. *Int J Oncol*. 2022;60(6):66. doi:10.3892/ijo.2022.5356
26. Liu X, Cai Y, Cheng C, et al. PCLAF promotes neuroblastoma G1/S cell cycle progression via the E2F1/PTTG1 axis. *Cell Death Dis*. 2022;13(2):178. doi:10.1038/s41419-022-04635-w
27. Wang K, Li J, Zhou B. KIAA0101 knockdown inhibits glioma progression and glycolysis by inactivating the PI3K/AKT/mTOR pathway. *Metab Brain Dis*. 2022;37(2):489–499. doi:10.1007/s11011-021-00863-9
28. Chorro L, Sarde A, Li M, et al. Langerhans cell (LC) proliferation mediates neonatal development, homeostasis, and inflammation-associated expansion of the epidermal LC network. *J Exp Med*. 2009;206(13):3089–3100. doi:10.1084/jem.20091586
29. Nedoszytko B, Sokołowska-Wojdyło M, Ruckemann-Dziurdzińska K, Roszkiewicz J, Nowicki RJ. Chemokines and cytokines network in the pathogenesis of the inflammatory skin diseases: atopic dermatitis, psoriasis and skin mastocytosis. *Postepy Dermatol Alergol*. 2014;31(2):84–91. doi:10.5114/pdia.2014.40920
30. Marschall P, Wei R, Segaud J, et al. Dual function of Langerhans cells in skin TSLP-promoted T(FH) differentiation in mouse atopic dermatitis. *J Allergy Clin Immunol*. 2021;147(5):1778–1794. doi:10.1016/j.jaci.2020.10.006
31. Toriyama M, Rizaldy D, Nakamura M, et al. Dendritic cell proliferation by primary cilium in atopic dermatitis. *Front mol Biosci*. 2023;10:1149828. doi:10.3389/fmolb.2023.1149828

32. Szabó K, Gáspár K, Dajnoki Z, et al. *Expansion of Circulating Follicular T Helper Cells Associates With Disease Severity in Childhood Atopic Dermatitis*. Vol. 189. Immunol Lett; 2017:101–108.
33. Jiang J, Yan S, Zhou X, et al. Crosstalk between circulating follicular t helper cells and regulatory B cells in children with extrinsic atopic dermatitis. *Front Immunol*. 2021;12:785549. doi:10.3389/fimmu.2021.785549
34. Das P, Mounika P, Yellurkar ML, et al. Keratinocytes: an enigmatic factor in atopic dermatitis. *Cells*. 2022;11(10):1683. doi:10.3390/cells11101683
35. Liu L, Michowski W, Kolodziejczyk A, Sicinski P. The cell cycle in stem cell proliferation, pluripotency and differentiation. *Nat Cell Biol*. 2019;21 (9):1060–1067. doi:10.1038/s41556-019-0384-4
36. Gupta VK, Chaudhuri O. Mechanical regulation of cell-cycle progression and division. *Trends Cell Biol*. 2022;32(9):773–785. doi:10.1016/j. tcb.2022.03.010
37. Liu X, Zhu R, Luo Y, et al. Distinct human Langerhans cell subsets orchestrate reciprocal functions and require different developmental regulation. *Immunity*. 2021;54(10):2305–2320. doi:10.1016/j.immuni.2021.08.012
38. Xu X, Dennett P, Zhang J, et al. CTLA4 depletes T cell endogenous and trogocytosed B7 ligands via cis-endocytosis. *J Exp Med*. 2023;220(7): e20221391. doi:10.1084/jem.20221391
39. Talagas M, Lebonvallet N, Berthod F, Misery L. Lifting the veil on the keratinocyte contribution to cutaneous nociception. *Protein Cell*. 2020;11 (4):239–250. doi:10.1007/s13238-019-00683-9
40. Medek K, Klausegger A, Ude-Schoder K, et al. Phenotypic alleviation in LAMB3-mutated severe junctional epidermolysis bullosa. *J Eur Acad Dermatol Venereol*. 2022;36(8):e631–e634. doi:10.1111/jdv.18091
41. O'connell P. Of LAMA3 and LAMB3: a novel gene therapy for epidermolysis bullosa. *mol Ther*. 2024;32(5):1197–1198. doi:10.1016/j. ymthe.2024.04.014
42. Huang Y, Zhao H, Zhang Y, et al. Enhancement of zyxin promotes skin fibrosis by regulating FAK/PI3K/AKT and TGF-β signaling pathways via integrins. *Int J Biol Sci*. 2023;19(8):2394–2408. doi:10.7150/ijbs.77649
43. Chovatiya R. Atopic dermatitis (Eczema). *JAMA*. 2023;329(3):268. doi:10.1001/jama.2022.21457
44. Zhang Y, Wang M, Li Z, et al. An overview of detecting gene-trait associations by integrating GWAS summary statistics and eQTLs. *Sci China Life Sci*. 2024;67(6):1133–1154. doi:10.1007/s11427-023-2522-8
45. Ding Q, Xu Q, Hong Y, et al. Integrated analysis of single-cell RNA-seq, bulk RNA-seq, Mendelian randomization, and eQTL reveals T cell-related nomogram model and subtype classification in rheumatoid arthritis. *Front Immunol*. 2024;15:1399856. doi:10.3389/fimmu.2024.1399856
46. Liu LJ, Liao JM, Zhu F. Proliferating cell nuclear antigen clamp associated factor, a potential proto-oncogene with increased expression in malignant gastrointestinal tumors. *World J Gastrointest Oncol*. 2021;13(10):1425–1439. doi:10.4251/wjgo.v13.i10.1425
47. Kolur V, Vastrad B, Vastrad C, Kottursheti S, Tengli A. Identification of candidate biomarkers and therapeutic agents for heart failure by bioinformatics analysis. *BMC Cardiovasc Disord*. 2021;21(1):329. doi:10.1186/s12872-021-02146-8
48. Wang C, Beylerli O, Gu Y, et al. Bioinformatics analysis screening and identification of key biomarkers and drug targets in human glioblastoma. *Curr Med Chem*. 2024.
49. Stopka-Farooqui U, Stavrinides V, Simpson BS, et al. Combining tissue biomarkers with mpMRI to diagnose clinically significant prostate cancer. Analysis of 21 biomarkers in the PICTURE study. *Prostate Cancer Prostatic Dis*. 2024. doi:10.1038/s41391-024-00920-1
50. Ferrari De Andrade L, Kumar S, Luoma AM, et al. Inhibition of MICA and MICB SHEDDING ELICIts NK-cell-mediated immunity against tumors resistant to cytotoxic T cells. *Cancer Immunol Res*. 2020;8(6):769–780. doi:10.1158/2326-6066.CIR-19-0483
51. Wu YQ, Cai YX, Chen XL, Chen SQ, Huang XF, Lin ZL. Proteomic analysis reveals potential therapeutic targets for childhood asthma through Mendelian randomization. *Clin Transl Allergy*. 2024;14(5):e12357. doi:10.1002/clt2.12357
52. Hervier B, Ribon M, Tarantino N, et al. Increased concentrations of circulating soluble MHC class I-related chain A (sMICA) and sMICB and modulation of plasma membrane MICA expression: potential mechanisms and correlation with natural killer cell activity in systemic lupus erythematosus. *Front Immunol*. 2021;12:633658. doi:10.3389/fimmu.2021.633658
53. Vorwerk G, Zahn S, Bieber T, Wenzel J. NKG2D and its ligands as cytotoxic factors in cutaneous lupus erythematosus. *Exp Dermatol*. 2021;30 (6):847–852. doi:10.1111/exd.14311
54. Capulli M, Olstad OK, Onnerfjord P, et al. The C-terminal domain of chondroadherin: a new regulator of osteoclast motility counteracting bone loss. *J Bone Miner Res*. 2014;29(8):1833–1846. doi:10.1002/jbmr.2206
55. Lucarini E, Nocentini A, Bonardi A, et al. Carbonic anhydrase IV selective inhibitors counteract the development of colitis-associated visceral pain in rats. *Cells*. 2021;10(10):2540. doi:10.3390/cells10102540